

## Electronic supplementary information

### Efficient and Stable All-Inorganic Perovskite Solar Cells Based on Nonstoichiometric $\text{Cs}_x\text{PbI}_2\text{Br}_x$ ( $x>1$ ) Alloys

Lyubov A. Frolova, Qing Chang, Sergey Yu. Luchkin, Daming Zhao, Azat F. Akbulatov,  
Nadezhda N. Dremova, Andrey V. Ivanov, Elbert E. M. Chia, Keith J. Stevenson, and Pavel  
A. Troshin

#### Contents

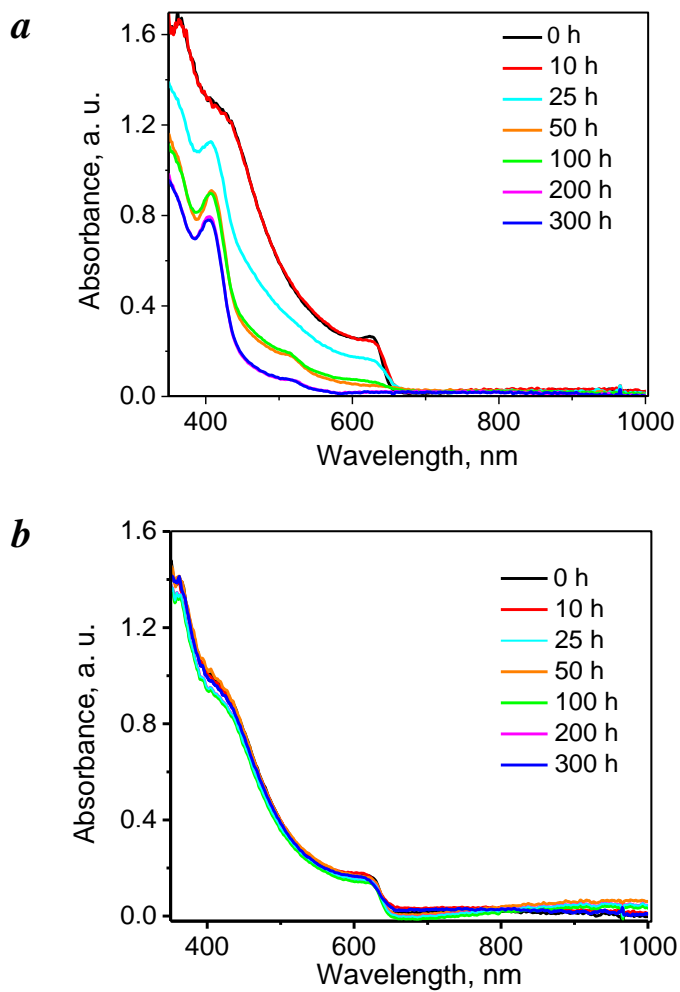
Fig. S1. Evolution of the absorption spectra of the perovskite thin films exposed to white light illumination (metal-halogen lamps,  $100 \text{ mW/cm}^2$ ) at  $70^\circ\text{C}$  in inert atmosphere for the material with the stoichiometric composition  $\text{CsPbI}_2\text{Br}$  (a) and the non-stoichiometric alloy  $\text{Cs}_{1.2}\text{PbI}_2\text{Br}_{1.2}$  (b).

Fig. S2. Best and average open circuit voltage (a), short circuit current density (b), and fill factor (c) of the devices based on the  $\text{Cs}_x\text{PbI}_2\text{Br}_x$  films with different compositions extracted from  $J$ - $V$  measurements (scan rate of  $0.1 \text{ V/s}$  in forward direction).

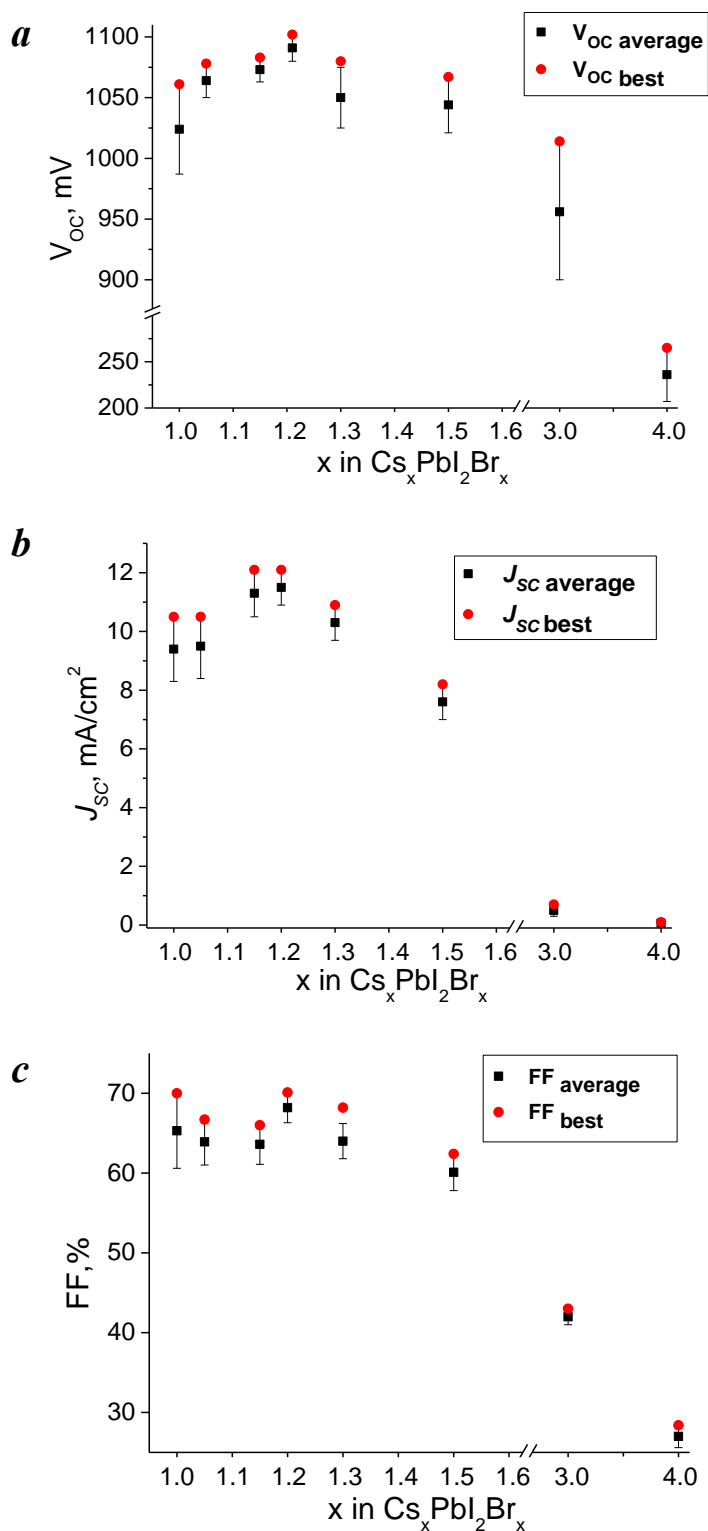
Fig. S3. Steady-state photocurrent measurements under constant load near the device maximal power point at  $V_{\text{max}}$  of  $760 \text{ mV}$ .

Fig. S4. Histograms of the maximum photocurrent distribution from  $I$ - $V$  measurements for the  $\text{CsPbI}_2\text{Br}$  (a) and  $\text{Cs}_{1.2}\text{PbI}_2\text{Br}_{1.2}$  (b) films.

Table S1. Average Cs/Pb atomic ratio in the deposited  $\text{Cs}_x\text{PbI}_2\text{Br}_x$  films according to flame atomic absorption spectrometry.



**Figure S1.** Evolution of the absorption spectra of the stoichiometric  $\text{CsPbI}_2\text{Br}$  (a) and non-stoichiometric  $\text{Cs}_{1.2}\text{PbI}_2\text{Br}_{1.2}$  (b) thin films exposed to white light illumination ( $100 \text{ mW/cm}^2$ ) at  $70^\circ \text{C}$  in inert atmosphere ( $\text{O}_2$ ,  $\text{H}_2\text{O} < 0.1 \text{ ppm}$ ).



**Figure S2.** Best and average open circuit voltage (a), short circuit current density (b), and fill factor (c) of the devices based on the  $\text{Cs}_x\text{PbI}_2\text{Br}_x$  films with different compositions extracted from  $J$ - $V$  measurements (scan rate of 0.1 V/s in forward direction).

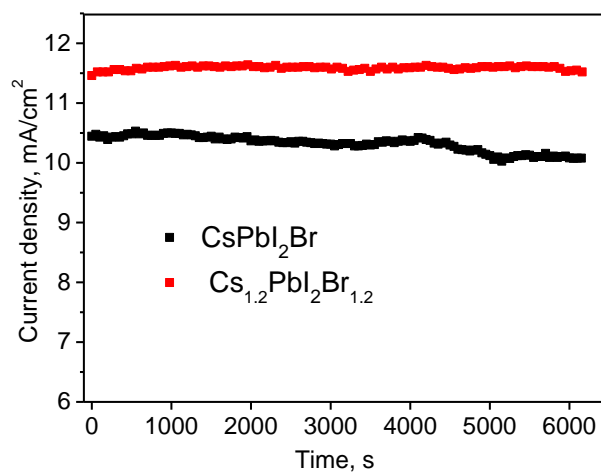


**Figure S3.** Steady-state photocurrent measurements under constant load near the device maximal power point at  $V_{\text{max}}$  of 760 mV.

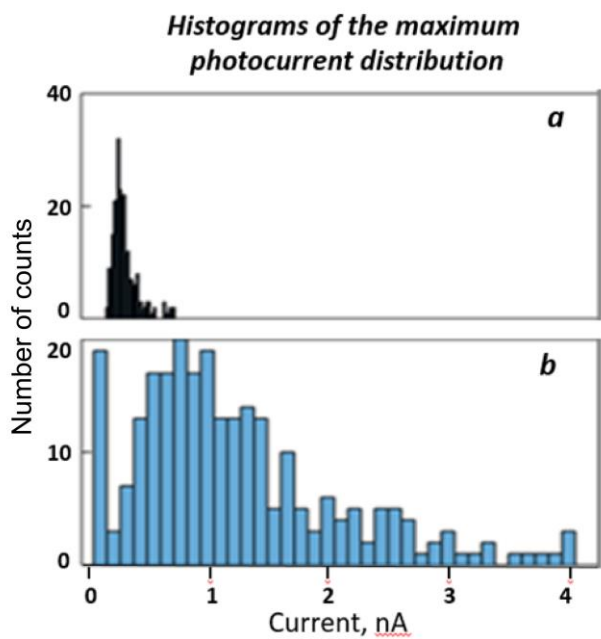


**Figure S4.** Histograms of the maximum photocurrent distribution from I-V measurements for the CsPbI<sub>2</sub>Br (a) and Cs<sub>1.2</sub>PbI<sub>2</sub>Br<sub>1.2</sub> (b) films.

**Table S1.** Average Cs/Pb atomic ratio in the deposited  $\text{Cs}_x\text{PbI}_2\text{Br}_x$  films according to flame atomic absorption spectrometry (AAS).

Composition of the films as defined by the thicknesses of CsBr and $\text{PbI}_2$	Cs/Pb atomic ratio experimentally determined using AAS*
$\text{Cs}_{0.95}\text{PbI}_2\text{Br}_{0.95}$	0.95
$\text{CsPbI}_2\text{Br}$	1.02
$\text{Cs}_{1.05}\text{PbI}_2\text{Br}_{1.05}$	1.07
$\text{Cs}_{1.15}\text{PbI}_2\text{Br}_{1.15}$	1.15
$\text{Cs}_{1.2}\text{PbI}_2\text{Br}_{1.2}$	1.18
$\text{Cs}_{1.3}\text{PbI}_2\text{Br}_{1.3}$	1.36
$\text{Cs}_{1.5}\text{PbI}_2\text{Br}_{1.5}$	1.50
$\text{Cs}_{3.0}\text{PbI}_2\text{Br}_{3.0}$	3.02
$\text{Cs}_{4.0}\text{PbI}_2\text{Br}_{4.0}$	3.93

\* - The relative standard deviations of the measurements were within 1%.